Periodic orbits of the retrograde coorbital problem

M. Morais, F. Namouni

Monthly Notices
of the
ROYAL ASTRONOMICAL SOCIETY

MNRAS **490,** 3799–3805 (2019)
Advance Access publication 2019 October 14

doi:10.1093/mnras/stz2868

Periodic orbits of the retrograde coorbital problem

M. H. M. Morais [1]★ and F. Namouni [2]

[1]*Instituto de Geociências e Ciências Exatas, Universidade Estadual Paulista (UNESP), Av. 24-A, 1515, 13506-900 Rio Claro, SP, Brazil*
[2]*CNRS, Observatoire de la Côte d'Azur, Université Côte d'Azur, CS 24229, F-06304 Nice, France*

Accepted 2019 October 8. Received 2019 October 7; in original form 2019 June 29

ABSTRACT

Asteroid (514107) Ka'epaoka'awela is the first example of an object in the 1/1 mean motion resonance with Jupiter with retrograde motion around the Sun. Its orbit was shown to be stable over the age of the Solar system, which implies that it must have been captured from another star when the Sun was still in its birth cluster. Ka'epaoka'awela orbit is also located at the peak of the capture probability in the coorbital resonance. Identifying the periodic orbits that Ka'epaoka'awela and similar asteroids followed during their evolution is an important step towards precisely understanding their capture mechanism. Here, we find the families of periodic orbits in the two-dimensional retrograde coorbital problem and analyse their stability and bifurcations into three-dimensional periodic orbits. Our results explain the radical differences observed in 2D and 3D coorbital capture simulations. In particular, we find that analytical and numerical results obtained for planar motion are not always valid at infinitesimal deviations from the plane.

Key words: celestial mechanics – minor planets, asteroids: general.

1 INTRODUCTION

The Solar system contains only one known asteroid in coorbital resonance with a planet, Jupiter, that moves with a retrograde motion around the Sun: asteroid (514107) Ka'epaoka'awela (Morais & Namouni 2017; Wiegert, Connors & Veillet 2017). Large-scale numerical integrations of its past orbital evolution, including perturbations from the four giant planets and the Galactic tide, have shown that it has been at its current location since the end of planet formation 4.5 Gyr in the past. Since a retrograde orbit could not have formed from the material of the Sun's protoplanetary disc at that early epoch, Ka'epaoka'awela must have belonged to a different star system and was captured by our own when the Sun was still in its birth cluster (Namouni & Morais 2018b). Ka'epaoka'awela is thus the first known example of an interstellar long-term resident in the Solar system. Understanding exactly how it reached its current location is particularly important.

Coorbital retrograde resonance has been studied in the framework of the restricted three-body problem. Several stable planar and three-dimensional coorbital configurations or modes are known to exist (Morais & Namouni 2013, 2016). Simulations of retrograde asteroids radially and adiabatically drifting towards Jupiter's orbit showed that when retrograde motion is almost coplanar, capture occurs in the coorbital mode that corresponds to Ka'epaoka'awela's current orbit (Morais & Namouni 2016; Namouni & Morais 2018a). If motion is exactly coplanar, capture occurs in a distinct coorbital mode (Morais & Namouni 2016; Namouni & Morais 2018a). In order to understand such differences and characterize the path that Ka'epaoka'awela followed in its capture by Jupiter, we aim to identify the periodic orbits (POs) of retrograde coorbital motion in the three-body problem.

The importance of POs in the study of a dynamical system has been recognized since the seminal work of Poincaré. Stable POs are surrounded by islands of regular (quasi-periodic) motion, whereas chaos appears at the location of unstable POs (Hadjedemetriou 2006). In the N-body problem, POs are the solutions such that the relative distances between the bodies repeat over a period T (Henon 1974). They form continuous families and may be classified as (linearly) stable or unstable (Henon 1974; Hadjedemetriou 2006). In the circular restricted three-body problem (CR3BP) with a dominant central mass, these families may be resonant or non-resonant. The former correspond to commensurabilities between the orbital frequencies, whereas the latter correspond to circular solutions of the unperturbed (two-body) problem (Hadjedemetriou 2006).

In this article, we report on our search of POs in the CR3BP with a mass ratio $\mu = 10^{-3}$. In Section 2, we explain how we compute the families of POs and study their stability. In Section 3, we describe the families that exist in the 2D configuration and the bifurcations from planar families to the 3D configuration. In Section 4, we discuss how these results explain the differences observed in the 2D and 3D capture simulations. The conclusions of this study are presented in Section 5.

★ E-mail: helena.morais@unesp.br

2 COMPUTATION OF PERIODIC ORBITS

From the periodicity theorem of Roy & Ovenden (1955), symmetric periodic orbits (SPOs) in the *N*-body problem must fullfil two mirror configurations. In the CR3BP the possible mirror configurations are: (a) perpendicular intersection of the (x, z) plane; (b) perpendicular intersection of the x-axis. The SPOs may be classified according to the combinations of mirror configurations: (a)–(a); (b)–(b); (a)–(b) (Zagouras & Markellos 1977). Planar SPOs intersect the x-axis perpendicularly at times $T/2$ and T (Hadjedemetriou 2006).

Morais & Namouni (2013) showed that planar POs associated with the retrograde 1/1 resonance are symmetric and have multiplicity 2, i.e. they intersect the surface of section $y = 0$, perpendicularly ($\dot{x} = 0$) and with the same sign for $\dot{y}$, at $t = T/2$ and $t = T$. We use the following standard algorithm to find planar POs:

(i) A guess initial condition $(x_0, 0, 0, \dot{y}_0)$ is followed until the second intersection with the surface of section occurs within $|y| < \epsilon_0$ at time T.

(ii) If $|\dot{x}| < \epsilon$ then the initial conditions correspond to a PO with period T. A new search is started varying x_0 or $\dot{y}_0$. Otherwise, a differential correction is applied to x_0 or $\dot{y}_0$ and the procedure is repeated.

The variational equations have the general solution $\bar{\xi}(t) = \Delta(t)\bar{\xi}(0)$ where $\bar{\xi}(t)$ is the phase-space displacement vector at time t and $\Delta(t)$ is the six-dimensional state transition matrix. The eigenvalues of $\Delta(T)$ indicate if the PO with period T is linearly stable or unstable. Due to the symplectic property of the equations of motion these eigenvalues appear as reciprocal pairs $\lambda_i\lambda_i^* = 1$ ($i = 1, 2, 3$) and they may be real or complex conjugate. The periodicity condition implies that one pair of eigenvalues is $\lambda_1 = \lambda_1^* = 1$. The PO is linearly stable if the remaining pairs of eigenvalues are complex conjugate on the unit circle and unstable otherwise with instability increasing with the largest eigenvalue's absolute value (Hadjedemetriou 2006).

For planar motion, the state transition matrix, $\Delta_2(t)$, is four-dimensional. The horizontal stability index is $k_2 = \lambda_2 + \lambda_2^*$, where λ_2 and λ_2^* are the non-trivial eigenvalues of $\Delta_2(T)$. Stable planar POs have $-2 < k_2 < 2$. Change of stability occurs when $|k_2| = 2$ (or $\lambda_2 = \lambda_2^* = \pm 1$), which is often associated with bifurcation of a new family of POs.

The variational equations for displacements out of the plane and in the plane of motion are decoupled when $z = \dot{z} = 0$ (Hénon 1973) hence the evolution of $\bar{\xi}_z(t) = (\mathrm{d}z, \mathrm{d}\dot{z})$ is described by a two-dimensional state transition matrix, $\Delta_3(t)$. The vertical stability index is $k_3 = \lambda_3 + \lambda_3^*$ where λ_3 and λ_3^* are the eigenvalues of $\Delta_3(T)$. Motion around stable 2D POs is maintained when there are small deviations out of the plane only if the vertical stability index $-2 < k_3 < 2$. When this stability index reaches the critical value 2 (vertical critical orbit or vco) a bifurcation into a new family of 3D POs with the same multiplicity may occur (Hénon 1973; Ichtiaroglou & Michalodimitrakis 1980).

To find 3D SPOs that bifurcate from vcos we follow a procedure similar to Zagouras & Markellos (1977):

(i) Initial conditions corresponding to mirror configurations: (a): $(x_0, 0, z_0, 0, \dot{y}_0, 0)$; or (b): $(x_0, 0, 0, 0, \dot{y}_0, \dot{z}_0)$; are followed until the second intersection with the surface of section occurs within $|y| < \epsilon_0$ at time T.

(ii) If $|\dot{x}| < \epsilon$ and $|\dot{z}| < \epsilon$ (a) or $|\dot{x}| < \epsilon$ and $|z| < \epsilon$ (b) then the initial conditions correspond to a PO with period T and a new search is started. Otherwise, a differential correction is applied to two components of the initial condition vector and the procedure is repeated.

For 3D motion, the pairs of eigenvalues λ_i, λ_i^* ($i = 2, 3$) of $\Delta(T)$ are the roots of the characteristic polynomial $\lambda^4 + \alpha\lambda^3 + \beta\lambda^2 + \alpha\lambda + 1$ with $\alpha = 2 - Tr(\Delta(T))$, $2\beta = \alpha^2 + 2 - Tr(\Delta(T)^2)$ (Bray & Goudas 1967). They are complex conjugate on the unit circle (linear stability) if $\delta = (\alpha^2 - 4(\beta - 2)) > 0$ and $|p| = |(\alpha + \sqrt{\delta})|/2 < 2$, $|q| = |(\alpha - \sqrt{\delta})|/2 < 2$ (Zagouras & Markellos 1977). Change of stability with possible bifurcation into a new family of POs occurs when pairs of eigenvalues coallesce on the real axis while complex instability occurs when they collaesce on the unit circle and then move away from it (Heggie 1985).

The numerical integration of the CR3BP equations of motion and associated variational equations were done using the Bulirsch–Stoer algorithm with per step accuracy 10^{-13}. Distance and time were scaled by Jupiter's semimajor axis and orbital period. The computations for an individual test particle were stopped when the distance to a massive body was within its physical radius (taken equal to the Sun's and Jupiter's radius). They were also stopped when the heliocentric distance exceeded 3 times Jupiter's semimajor axis.

The thresholds for deciding if an orbit is periodic were chosen so that the differential correction procedure converges for each specific type of PO. We used $\epsilon_0 = 10^{-11}$ and $\epsilon = 10^{-10}$ to find planar and 3D POs. In general, lower (sometimes unfeasible) values are necessary to follow unstable families, as expected due to the exponential divergence of solutions close to unstable POs. To monitor the POs computations, we checked that $|\Delta(T)| = 1$ with at least 11 significant digits. Stability and bifurcation points were further checked by explicitly computing the eigenvalues of $\Delta(T)$. Unstable critical motion (near the transition to stability) was confirmed by computing the chaos indicator MEGNO (Cincotta & Giordano 2006).

3 THE 2D FAMILIES AND BIFURCATIONS INTO 3D

Morais & Namouni (2013) showed that the relevant resonant argument for planar retrograde coorbitals in the CR3BP is $\phi^* = \lambda - \lambda_p - 2\omega$ where λ and ω are the test particle's mean longitude and argument of pericentre, respectively, and λ_p is the mean longitude of the planet. There are three types of retrograde coorbitals: mode 1 which corresponds to libration of ϕ^* around 0 and occurs at a wide range of eccentricities; modes 2 and 3 which correspond to libration of ϕ^* around 180° and occur, respectively, at small eccentricity (mode 3) and large eccentricity (mode 2). These modes are retrieved in a 2D model for retrograde coorbital resonance based on the averaged Hamiltonian (Huang et al. 2018).

3.1 Planar SPOs

We show how the families of SPOs associated with mode 1 (Fig. 1) and modes 2 and 3 (Fig. 2) evolve with the Jacobi constant, C.

Mode 1 resonant POs are horizontally stable when $C > -1.2256$ and vertically stable when $C > -1.0507$ ($a < 1.0380$, $e > 0.1125$). The family ends by collision with the star when $e \approx 1$.

Inner nearly circular non-resonant POs are stable if $C > -0.8429$ ($a < 0.9265$). At $C = -0.9562$ ($a = 0.9801$) there is a bifurcation into a stable inner resonant PO. This family is stable up to $C = -0.8643$ ($a = 0.9864$, $e = 0.3208$: inner mode 3) and stable again from $C = -0.3349$ ($a = 0.9976$, $e = 0.7411$: mode 2). Therefore, mode 2 and inner mode 3 resonant POs form a single family which

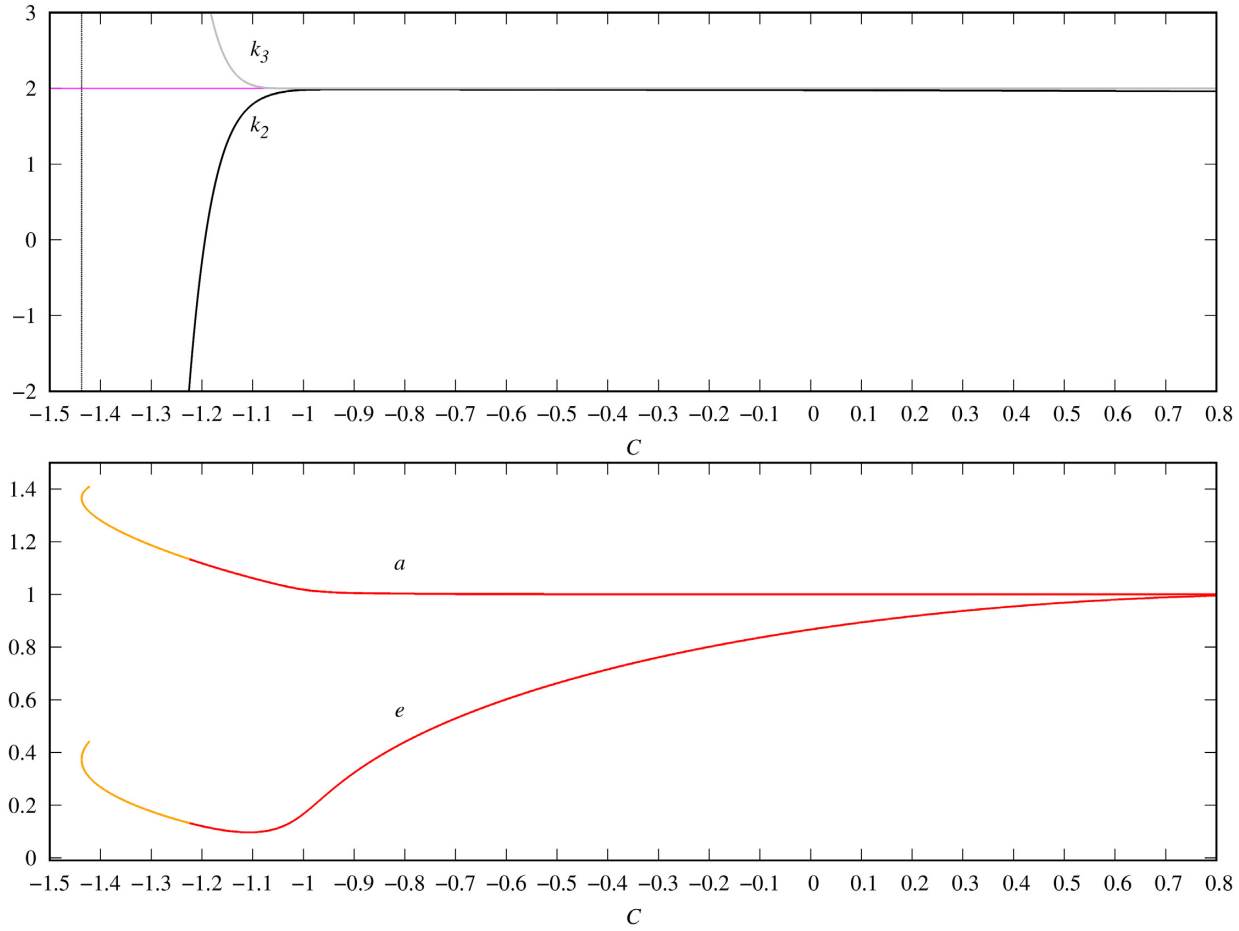

Figure 1. Family of SPOs corresponding to retrograde mode 1 with respect to the Jacobi constant, C. Top panel: 2D (black) and 3D (grey) stability indexes. Low panel: semimajor axis a and eccentricity e [horizontally stable (red) and unstable (orange)].

is always vertically stable. The family ends by collision with the star when $e \approx 1$.

Outer nearly circular non-resonant POs are vertically unstable when $-1.0395 > C > -1.1499$ ($1.0218 < a < 1.0804$). At $C = -1.0387$ ($a = 1.0215$) there is a bifurcation into a pair of stable (outer mode 3) and unstable POs. Outer mode 3 resonant POs are stable up to $C = -0.9553$ ($a = 1.0151$, $e = 0.2636$).

3.2 Bifurcations into 3D

Morais & Namouni (2013) and Morais & Namouni (2016) showed that in the 3D coorbital problem the relevant resonant angles are $\phi = \lambda - \lambda_p$ and $\phi^* = \lambda - \lambda_p - 2\omega$. The 3D retrograde coorbital modes correspond to: ϕ librating around 180° (mode 4); ϕ^* librating around 0 (mode 1) or 180° (modes 2 and 3).

Planar retrograde modes 1 and 2 are horizontally and vertically stable when $C > -1.0507$ and $C > -0.3349$, respectively, hence the associated POs are surrounded by quasi-POs in the 3D problem. In particular, quasi-periodic mode 1 and mode 2 orbits may extend down to inclinations $i = 90°$ and $i = 120°$, respectively (Morais & Namouni 2016).

The vertical critical orbits (vcos) occur: on mode 1 family at $C = -1.0507$ (Fig. 1); on the outer circular family at $C = -1.1499$ and $C = -1.0395$ (Fig. 2). At the vcos there are bifurcations into new families of 3D POs which we show in Fig. 3. The mode 2, mode 3 outer and inner families have no vcos as the vertical stability index, $k_3 < 2$.

At $C = -1.1499$ there is a bifurcation of a nearly circular 2D outer PO into a stable 3D resonant PO on configuration (b) which corresponds to mode 4 (libration centre $\phi = 180°$). This family reaches critical stability at $C = -1.0321$ when $i \approx 173°$. Fig. 4 shows a PO at this point on the family. Initially, $\phi = 180°$ with ω circulating fast similarly to mode 4 stable branch (Fig. 4: left). The peaks in a and e occur twice per period, at the encounters with the planet. After $t = 8 \times 10^3$, chaotic diffusion is obvious (MEGNO increases linearly with time) and from $t = 1.8 \times 10^4$ there are transitions between libration around $\omega = 90°$, 270° at small e when $\phi = 180°$ and circulation around the Kozai centres $\omega = 0$, 180° with eccentricity oscillations up to $e = 0.14$ (Fig. 4: right) when ϕ circulates. The Kozai circles around $\omega = 0$, 180° raise the eccentricity and shift the libration centre to $\phi^* = 0$.

At $C = -1.0507$ there is a bifurcation of planar mode 1 into a 3D PO on configuration (a). This family is unstable but nearly critical. It has a v-shape with lower / upper branches corresponding the intersection with the surface of section at the apocentric / pericentric encounters (Fig. 6: left). There is a bifurcation at $C = -1.0321$ coinciding with the bifurcation on the mode 4 family. Fig. 5 shows a PO at this bifurcation point. Initially, $\phi = 180°$ with ω circulating fast (Fig. 5: left). After $t = 7 \times 10^3$, chaotic diffusion is again obvious (Fig. 5: right) with the same qualitative behaviour observed in Fig. 4.

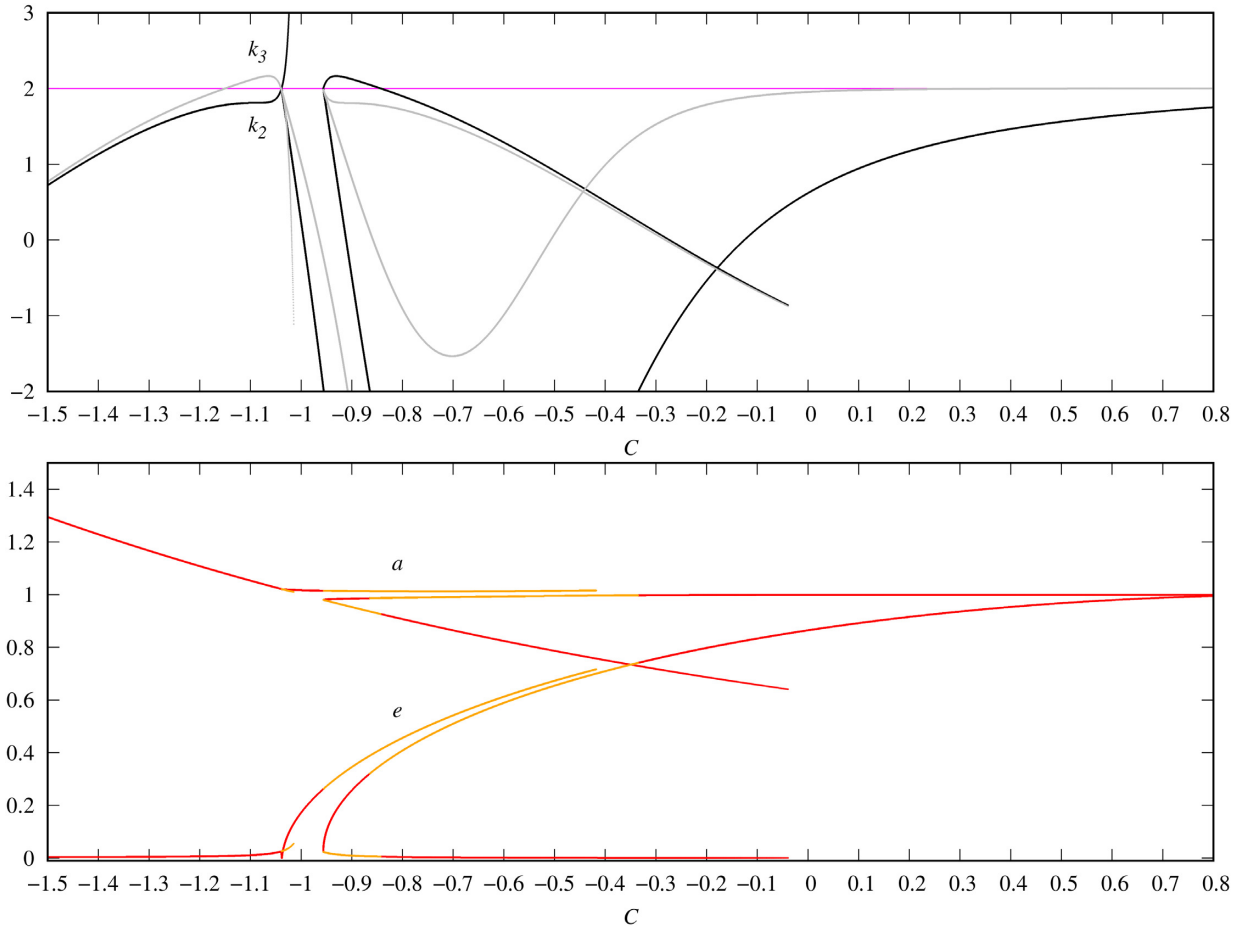

Figure 2. Family of SPOs corresponding to the outer and inner circular families and retrograde modes 2 and 3 with respect to the Jacobi constant, C. Top panel: 2D (black) and 3D (grey) stability indexes. Low panel: semimajor axis a and eccentricity e [horizontally stable (red) and unstable (orange)].

A shift of $t = 0.25$ between the time series in Figs 4 and 5 (left) causes overlap of orbital elements. Further inspection shows that they correspond to the same PO of symmetry type (a)–(b) at different intersections with the surface of section (Fig. 6: right). Hence, the 3D families bifurcating from the vcos at $C = -1.1499$ and $C = -1.0507$ join at $C = -1.0321$ generating a single unstable circular family which could be continued to $i \approx 8^\circ$ and $a = 0.999$. Since instability on this family increases sharply with decreasing inclination the differential correction scheme stops converging preventing further continuation. We suspect that termination occurs at the Lagrangian point L3 when $i = 0$ which is further supported by the shape of the last computed PO in the rotating frame.

At $C = -1.0395$, near the end of the stable branch of the 2D nearly circular outer family, there is a bifurcation into an unstable 3D PO on configuration (a). This 3D family corresponds to an unstable fixed point of the coorbital resonance Hamiltonian ($\phi = 0$ and $\phi^\star = 180^\circ$). It could be continued to $i \approx 88^\circ$, $e \approx 0.80$, and $a = 1.001$ at which point the family is approaching critical stability. However, the long integration of the initial conditions that approximate the last computed PO shows that the eccentricity increases sharply towards unity around $t = 5 \times 10^3$ thus leading to collision with the star. The proximity of the collision singularity prevents further continuation of the family.

4 COORBITAL CAPTURE IN 2D AND 3D CASES

In the planar problem, outer orbits slowly approaching the planet follow the nearly circular non-resonant family which bifurcates into a resonant SPO at $C = -1.0387$ when $a = 1.0215$ (outer mode 3). Capture into outer mode 3 occurs with probability 1 in agreement with Namouni & Morais (2018a) but the family becomes unstable at $C = -0.9553$ when $a = 1.0151$ and $e = 0.2636$.

However, Fig. 3 shows that the behaviour in the (real) 3D problem at infinitesimal deviations from the plane is radically different. The nearly circular non-resonant family is vertically unstable between $-1.0395 > C > -1.1499$. The vco at $C = -1.1499$ ($a = 1.0804$) bifurcates into a resonant mode 4 stable 3D family. Hence, outer circular orbits slowly approaching the planet still follow initially the non-resonant family which bifurcates into the 3D mode 4 family. The inclination then decreases and at $i \approx 173^\circ$ mode 4 family becomes unstable. At this point, mode 4 family connects with the critical 3D family which bifurcates from the vco at $C = -1.0507$ ($a = 1.0380$, $e = 0.1125$) on the stable branch of the mode 1 planar family. Chaotic transition between the Kozai centres located at $\omega = 90^\circ$, 270° and the separatrices around $\omega = 0$, 180° are accompanied by eccentricity oscillations up to 0.14 and a shift of

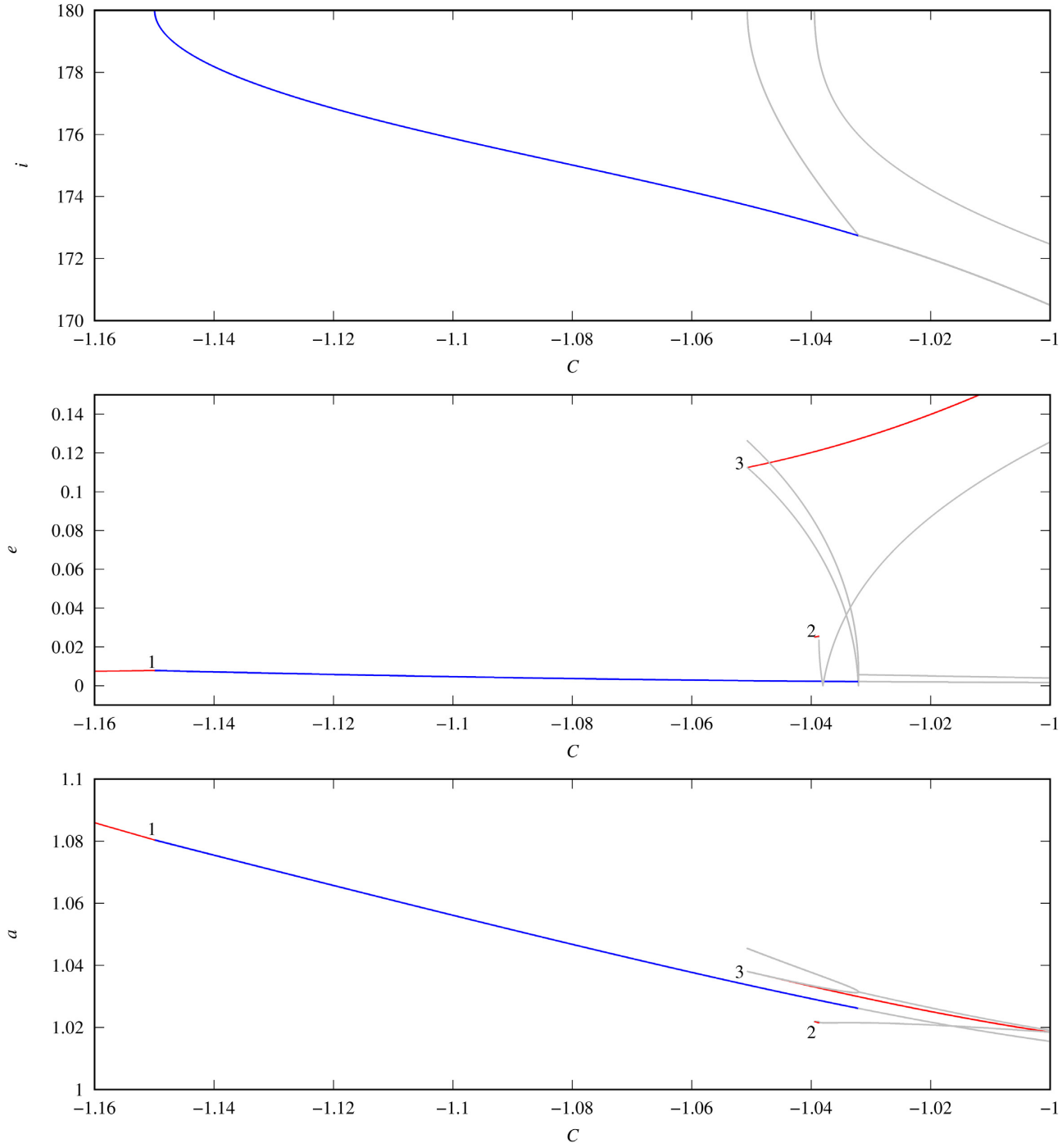

Figure 3. Families of 3D POs bifurcating from the vcos at $C = -1.1499$ and $C = -1.0395$ on the outer nearly circular family and $C = -1.0507$ on the planar mode 1 family. These vcos are labelled 1, 2, and 3, respectively. Top panel: inclination i. Mid-panel: eccentricity e. Low panel: semimajor axis a. The families are coloured blue (grey) when stable (unstable). The 2D stable families from which the 3D families bifurcate are coloured red.

the libration centre towards $\phi^* = 0$. Exit of this chaotic region due to a slow decrease in semimajor axis allows permanent capture into a quasi-periodic mode 1 orbit, in agreement with the simulations by Morais & Namouni (2016), Namouni & Morais (2018a).

Inner circular orbits slowly approaching the planet near the plane become horizontally unstable at $C = -0.8429$ when $a = 0.9265$. Therefore, the inner mode 3 resonant family cannot be reached (Morais & Namouni 2016). The resonant family starts at $C = -0.9562$ ($a = 0.9801$: inner mode 3), becomes horizontally unstable at $C = -0.8643$ ($a = 0.9864$, $e = 0.3208$) and is stable again when $C > -0.3349$ ($a > 0.9976$, $e > 0.7411$: mode 2). There are no vcos on the inner families.

5 CONCLUSION

We showed how the families of POs for the planar retrograde coorbital problem and their bifurcations into 3D explain the radical differences seen in our capture simulations, namely why 2D orbits

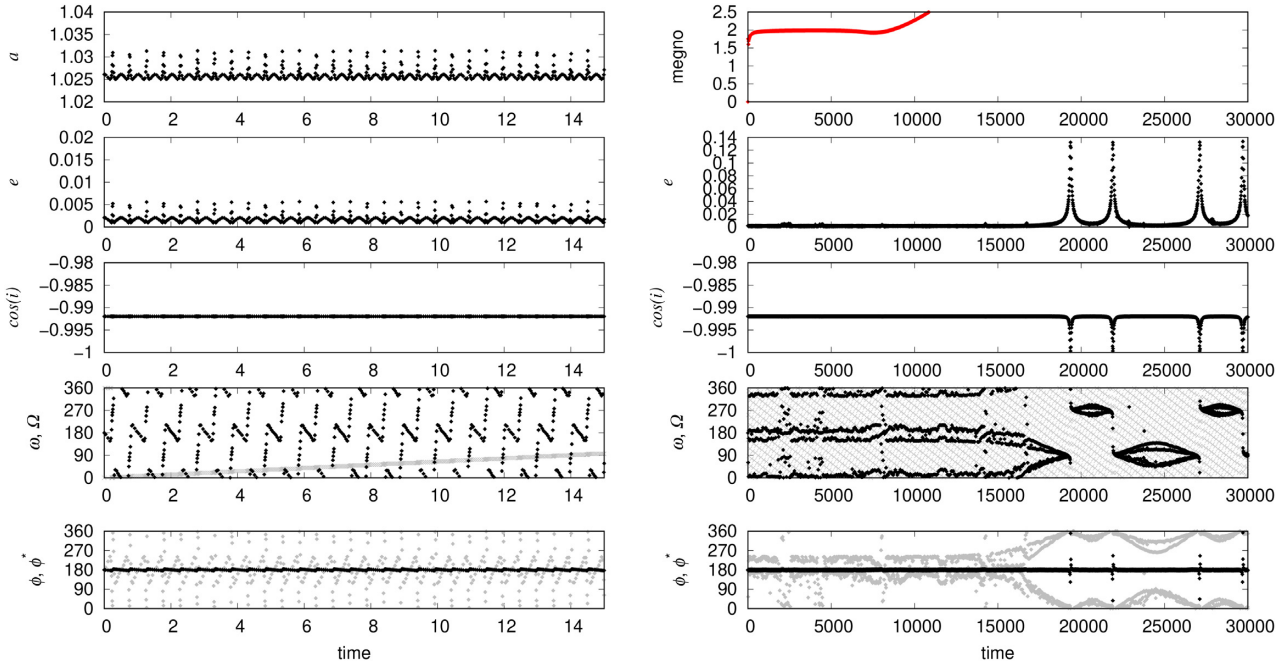

Figure 4. Evolution of PO at the critical point ($C = -1.0321$) on the 3D mode 4 family. From top to bottom panels: semimajor axis/MEGNO; eccentricity, cosine of inclination, argument of pericentre ω (black) and longitude of ascending node Ω (grey); resonant angles ϕ (black) and ϕ^* (grey).

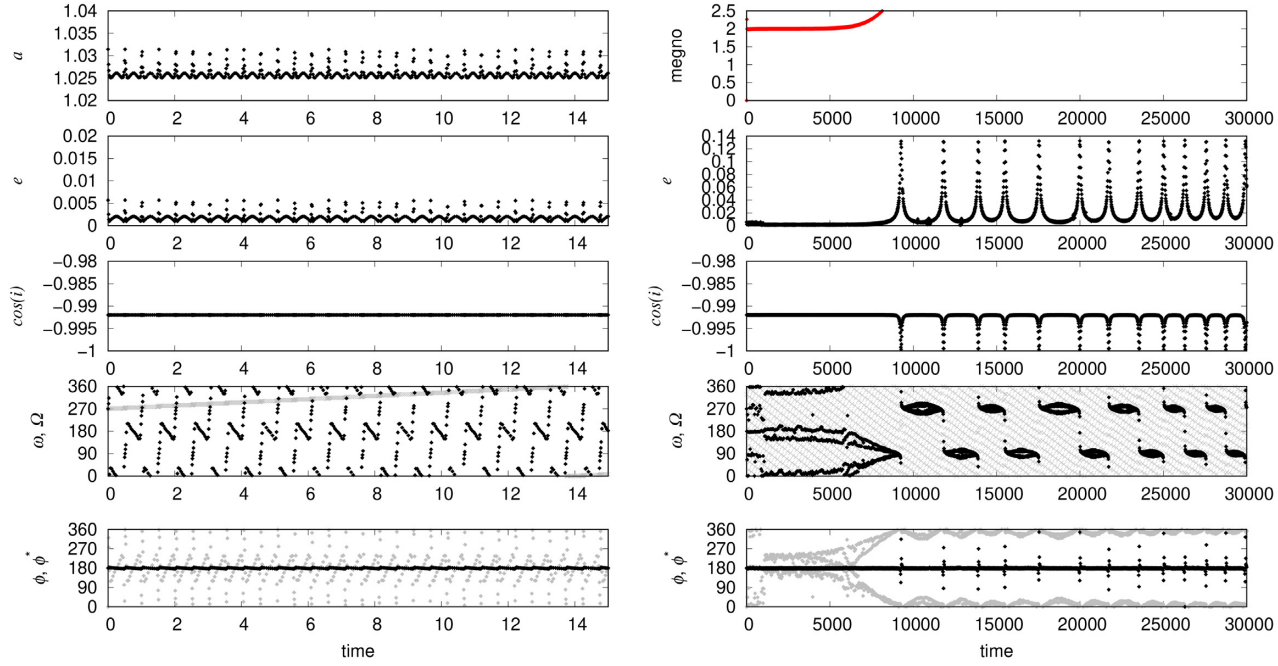

Figure 5. Evolution of PO at the critical point ($C = -1.0321$) on the 3D family which bifurcates from the vco on the planar mode 1 family. Same panels as Fig. 4.

are captured into mode 3 while 3D orbits are captured into mode 1 (Morais & Namouni 2016). In the planar problem, outer circular orbits slowly drifting towards the planet follow the non-resonant family which bifurcates into a resonant mode 3 family at $C = -1.0387$ ($a = 1.0215$). This family becomes unstable at $C = -0.9553$ ($a = 1.0151$, $e = 0.2636$). However, in the (real) 3D problem, mode 3 orbits are never reached. The nearly circular 2D family becomes vertically unstable (vco) at $C = -1.1499$ when $a = 1.0804$ where a bifurcation into a 3D resonant family corresponding to mode 4 ($\phi = 180^\circ$) occurs. This family becomes unstable when $i \approx 173^\circ$ as it connects with a 3D family bifurcating from the vco on mode 1 ($\phi^* = 0$). Chaotic transitions between the libration centres $\phi = 180^\circ$ and $\phi^* = 0$ are associated with motion in the vicinity of Kozai separatrices. As the semimajor axis decreases due to dissipation there is capture on a mode 1 inclined quasi-PO, similar to that of Ka'epaoka'awela.

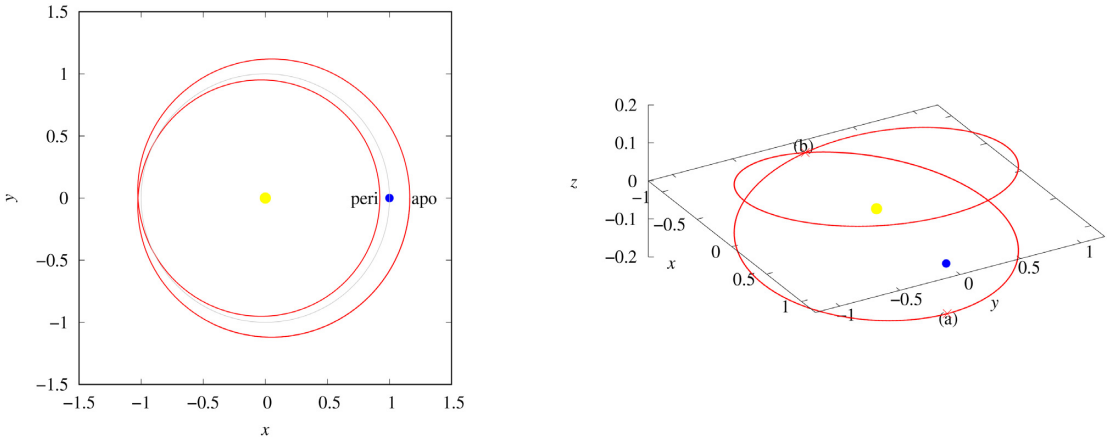

Figure 6. POs in rotating frame: (left) mode 1 vco has encounters and intersections with the surface of section at pericentre or apocentre; (right) 3D bifurcation at $C = -1.0321$ (mirror configurations a and b are shifted by $t = 0.25$).

Our results explain why mode 1 is the likely end state for objects on retrograde outer circular orbits slowly drifting towards the planet. If the planet migrated inwards, retrograde inner nearly circular orbits become horizontally unstable at $C = -0.8427$ when $a = 0.9265$ hence capture into inner mode 3 is not possible. However, eccentric inner retrograde orbits could be captured directly into mode 2 if the relative semimajor axis evolved in discrete steps. Similarly, eccentric outer orbits may be captured directly into mode 1. This could occur e.g. if the semimajor axis evolves stochastically due to planetary close approaches (Carusi, Valsecchi & Greenberg 1990). In the early Solar system the latter mechanism (outer eccentric capture) is more likely to occur than the former (inner eccentric capture) and this could explain how Ka'epaoka'awela arrived at the current location.

Analytical and numerical results obtained in 2D models are often thought to be valid when the motion is almost coplanar. Here, we showed that such extrapolation is not valid for the retrograde coorbital problem. This is due to the vertical instability of the nearly circular 2D family of POs. A similar mechanism has been reported for the 2/1 and 3/1 prograde resonances in the planetary (non-restricted) three-body problem (Voyatzis, Antoniadou & Tsiganis 2014).

Searches for 3D POs typically show that families end by collision with one of the massive bodies or otherwise exist over the entire inclination range $0 \leq i \leq 180^\circ$ (Kotoulas & Voyatzis 2005; Antoniadou & Libert 2019). Here, we computed the families that originate at the vcos of the planar retrograde coorbital problem. The family corresponding to an unstable fixed point of the coorbital Hamiltonian ($\phi = 0, \phi^\star = 180^\circ$) could be continued until it becomes a nearly polar orbit in the vicinity of an instability that leads to collision with the star. The unstable doubly symmetric circular family corresponding to the libration centre $\phi = 180^\circ$ seems to end at the collinear Lagrangian point L3. However, as this family becomes increasingly unstable as the inclination approaches zero its exact termination could not be ascertained.

ACKNOWLEDGEMENTS

Bibliography access was provided by CAPES-Brazil. MHMM research had financial support from São Paulo Research Foundation (FAPESP/2018/08620-1) andCNPq-Brazil (PQ2/304037/2018-4).

REFERENCES

Antoniadou K. I., Libert A.-S., 2019, MNRAS, 483, 2923
Bray T. A., Goudas C. L., 1967, AJ, 72, 202
Carusi A., Valsecchi G. B., Greenberg R., 1990, Celest. Mech. Dyn. Astron., 49, 111
Cincotta P. M., Giordano C.M., 2016, in Skokos C. et al., eds, 915, Lecture Notes in Physics: Chaos detection and predictability. Springer-Verlag, p. 93
Hadjedemetriou J. D., 2006, in Steves B. A., Maciejewski A. J., Hendry M., eds, Chaotic Worlds: from order to disorder in gravitational n-body dynamical systems. Springer, The Netherlands, p. 43
Heggie D. C., 1985, Celest. Mech., 35, 357
Hénon M., 1973, Celest. Mech., 8, 269
Henon M., 1974, Celest. Mech., 10, 375
Huang Y., Li M., Li J., Gong S., 2018, AJ, 155, 262
Ichtiaroglou S., Michalodimitrakis M., 1980, A&A, 81, 30
Kotoulas T. A., Voyatzis G., 2005, A&A, 441, 807
Morais M. H. M., Namouni F., 2013, Celest. Mech. Dyn. Astron., 117, 405
Morais M. H. M., Namouni F., 2016, Celest. Mech. Dyn. Astron., 125, 91
Morais M. H. M., Namouni F., 2017, Nature, 543, 635
Namouni F., Morais M. H. M., 2018a, J. Comput. Appl. Math., 37, 65
Namouni F., Morais M. H. M., 2018b, MNRAS, 477, L117
Roy A. E., Ovenden M. W., 1955, MNRAS, 115, 296
Voyatzis G., Antoniadou K. I., Tsiganis K., 2014, Celest. Mech. Dyn. Astron., 119, 221
Wiegert P., Connors M., Veillet C., 2017, Nature, 543, 687
Zagouras C., Markellos V. V., 1977, A&A, 59, 79

This paper has been typeset from a TEX/LATEX file prepared by the author.